High-energy components and collective modes in thermonuclear plasmas

B. Coppi [a)]
Massachusetts Institute of Technology, Cambridge, Massachusetts 02139

S. Cowley and R. Kulsrud
Plasma Physics Laboratory, Princeton University, Princeton, New Jersey 08544

P. Detragiache and F. Pegoraro
Scuola Normale Superiore, 56100 Pisa, Italy

(Received 6 November 1985; accepted 29 August 1986)

The theory of a class of collective modes of a thermonuclear magnetically confined plasma, with frequencies in the range of the ion-cyclotron frequency and of its harmonics, is presented. These modes can be excited by their resonant cyclotron interaction with a plasma component of relatively high-energy particles characterized by a strongly anisotropic distribution in velocity space. Normal modes that are spatially localized by the inhomogeneity of the plasma density are found. This ensures that the energy gained by their resonant interaction is not convected away. The mode spatial localization can be significantly altered by the magnetic field inhomogeneity for a given class of plasma density profiles. Special attention is devoted to the case of a spin polarized plasma, where the charged products of fusion reactions are anisotropically distributed. It is shown that for the mode of polarization that enhances nuclear reaction rates the tritium will be rapidly depolarized for toroidal configurations with relatively mild gradients of the confining magnetic field.

I. INTRODUCTION

In a magnetically confined plasma, high-frequency collective modes (in the ion-cyclotron range of frequency) may be driven unstable by resonant interaction with a high-energy ion population. Energetic ion populations can arise in thermonuclear plasmas either as a result of the injection of fast neutral beams or, more fundamentally, as the charged products of the fusion reactions. The presence of nonthermal features in the energetic ion distribution functions, such as nonmonotonicity and/or anisotropy in velocity space or spatial inhomogeneity, can be the source of the excitation energy that is necessary to sustain the growth of the mode amplitude.

We note that an analysis of the mode spatial structure that takes into account the inhomogeneity of a realistic plasma configuration is necessary in order to ascertain the effective occurrence of this type of instability. In fact, the energy transfer rate between the energetic ions and the modes, as derived in the limit of a homogeneous plasma model, is typically a relatively small quantity. Thus energy convection, which is often an important factor in the instability of modes in inhomogeneous configurations, or damping processes attributable to the bulk plasma species, can significantly alter the energy balance.

In this paper we determine the conditions under which the high-frequency modes exist as radially localized normal modes in a toroidal configuration. The problem of the excitation of these modes in the case of a spin polarized plasma is then addressed, as it is of particular relevance for the investigations on the processes of nuclear spin depolarization. We recall that the interest in the physics of fusing plasmas with polarized nuclear spins has been rekindled recently by the analysis presented in Ref. 1. In particular, this analysis suggested that a thermonuclear plasma with coherently polarized nuclear spins could maintain its polarization for a time the order of, or longer than, the particle fusion time. Thus, control over the spin polarization of the fusing nuclei would give a series of advantages, ranging from a 50% enhancement[1] of the fusion rate in a D–T plasma to a more efficient confinement of the charged fusion reaction products. Additional advantages would be a more convenient redistribution of the neutron flux over the chamber walls, of relevance, for example, to the process of tritium breeding[2] in a lithium blanket, or possibly to the achievement of nearly neutron-free D–He^3 burning conditions,[3] although this possibility depends on the actual spin dependence of the D–D fusion cross section, which is still under debate.[4,5] An effective mechanism for causing a fast depolarization of the nuclear spin would be the possible presence in the plasma of collective magnetic fluctuations at a level above thermal. These can resonate with the nuclear spin precession frequency and thus induce spin–flip transitions (see Sec. VI). It was pointed out in Refs. 6 and 7 that magnetic fluctuations of this type can be excited in a polarized D–T plasma by an anisotropy in velocity space of the fusion produced α particles, this anisotropy being a consequence of the coherent polarization of the reacting D–T nuclei. In the present paper a detailed analysis of the conditions for such an excitation in an inhomogeneous configuration is presented. We find a characteristic value of the growth rate, divided by the mode frequency, of order 10^{-1} times the relative α-particle density. We also find that for devices with relatively large values of the inverse aspect ratio, the bulk ion-cyclotron damping can be important.

High-energy ion populations are also produced in present-day experiments where neutral beams are injected to provide auxiliary heating. In fact, enhanced fluctuations in

[a)] Also at Princeton University, Plasma Physics Laboratory, Princeton, New Jersey 08544.

 0031-9171/86/124060-13$01.90

the ion-cyclotron range of frequency have been recently observed in various devices during neutral beam injection experiments.[8,9] An application of our theory to this case, however, would require a detailed study of the hot-ion distribution function that results from neutral beam ionization processes and of its subsequent evolution. We consider this task beyond the scope of this paper. Our presentation is organized as follows.

In Sec. II, the relevant modes are discussed in the limit of a homogeneous plasma model. Two different frequency ranges are considered for a plasma with two bulk ion species. In the lower range, the mode frequency is the order of the ion-cyclotron frequency, and the dispersion relation is complicated by the presence of a cutoff and of a resonance frequency. In the upper range, the mode frequency corresponds to higher harmonics of the ion-cyclotron frequency, and the dispersion relation reduces to that of magnetosonic waves. Subsequently, the presence of mode–particle resonances with the high energy ions and with the bulk plasma species is considered, and the relevant expression for the growth (damping) rate is derived.

In Sec. III, the spatial structure of the modes is analyzed initially from a heuristic dispersion equation derived from the local dispersion relation given in Sec. II, and then by gradually increasing the level of complexity, first in a cylindrical and then in a toroidal configuration. In the upper frequency range we find that the radially localized normal mode solutions derived in a cylindrical configuration are also possible in a toroidal one, provided that the density profile does not belong to a given class. For density profiles in this case (of which a parabolic density profile is a remarkable example), the associated modes tend to drift out of the plasma column. In the lower frequency range the modes are found to be substantially damped by the resonant electrons (transit time damping).

In Sec. IV, we adopt the geometrical optics approximation to describe the normal mode solutions found in Sec. III and to give a relatively clear graphic representation of various significant cases.

In Sec. V, we evaluate the growth rate of the relevant modes in the case where the deuterium and tritium components of the fusing plasma are coherently spin polarized, and the distribution of the produced α particles is anisotropic in velocity space.

In Sec. VI, we evaluate the rate of spin depolarization as a function of the mode amplitude and find that, in the presence of excited modes, the depolarization of the tritium nuclei is as fast as the particle confinement time.

In Sec. VII, we summarize our conclusions.

II. HOMOGENEOUS MODEL

A. Mode features and dispersion relation

In this section, we refer to a homogeneous, magnetized plasma with two bulk ion species (for definiteness, we shall consider a deuterium–tritium plasma), in which a small population of high energy ions is also present (we shall use a subscript "h" to denote quantities referring to this "hot" population).

We look for electromagnetic modes that can interact resonantly with the high-energy ions and that are not damped, or at most only weakly damped, by the bulk plasma. Thus we consider modes with a frequency ω close to one of the harmonics of the hot ion-cyclotron frequency Ω_h, i.e., $\omega \simeq p\Omega_h$, where p is an integer, and with a wave vector component $k_\perp$ perpendicular to the equilibrium magnetic field $\mathbf{B}_0$, such that $k_\perp v_h/\Omega_h \simeq p$. Here, $v_h = (2\epsilon_h/m_h)^{1/2}$ is a characteristic velocity of the hot-ion distribution function, and ϵ_h is the corresponding energy. Further, in order to avoid significant parallel electron Landau damping and transit-time damping, we shall focus on modes that have a vanishing parallel electric field and propagate almost perpendicularly to $\mathbf{B}_0$.

We take the perpendicular fluctuating electric field to be of the form

$$\mathbf{E}_1(\mathbf{r},t) = \tilde{\mathbf{E}} \exp[-i(\omega t - k_\parallel z - k_\perp y)] \tag{1}$$

and describe the bulk plasma response using the cold plasma conductivity tensor $\boldsymbol{\sigma}$:

$$\boldsymbol{\sigma} = \begin{pmatrix} \sigma_\perp & 0 \\ 0 & \sigma_\parallel \end{pmatrix}. \tag{2}$$

Here small terms of order $(k_\parallel/k_\perp)^2, \omega/\Omega_e$, and m_e/m_i have been neglected, $\sigma_\parallel = i\omega_{pe}^2/(4\pi\omega)$ and

$$\boldsymbol{\sigma}_\perp = -\frac{i\sigma_0}{\omega}\begin{pmatrix} 1 & i\lambda \\ -i\lambda & 1 \end{pmatrix}, \quad \sigma_0 = -\frac{en_e c\omega^2}{B_0}\sum_{i=\mathrm{D,T}}\frac{\alpha_i\Omega_i}{\Omega_i^2-\omega^2}, \tag{3}$$

and the polarization factor $\lambda(\omega) = -i\tilde{E}_y/\tilde{E}_x$ is given by

$$\lambda(\omega) = \frac{\Sigma_{i=\mathrm{D,T}}\,\alpha_i\omega/(\Omega_i^2-\omega^2)}{\Sigma_{i=\mathrm{D,T}}\alpha_i\Omega_i/(\Omega_i^2-\omega^2)}, \tag{4}$$

with $\alpha_i = (n_i/n_e)$ the isotopic ratio. From Maxwell equations and Eq. (2) with $\tilde{E}_\parallel \cong 0$, we obtain

$$4\pi\sigma_0(1-\lambda^2) = k^2c^2, \tag{5}$$

which can be rewritten as[6,10]

$$K(\omega) \equiv \frac{\omega^2}{k^2\bar{v}_A^2}\frac{\omega^2-\bar{\Omega}^2}{\omega^2-\Omega_{\mathrm{Hy}}^2} = 1. \tag{6}$$

This dispersion relation describes magnetosonic (compressional, fast Alfvén) waves modified by the so-called ion–ion hybrid resonance that occurs in a plasma with more than one ion species. The cutoff frequency $\bar{\Omega}$ and the resonance frequency Ω_{Hy} are defined by $\bar{\Omega} = \alpha_\mathrm{D}\Omega_\mathrm{T} + \alpha_\mathrm{T}\Omega_\mathrm{D}$ and $\Omega_{\mathrm{Hy}} = (\Omega_\mathrm{D}\Omega_\mathrm{T}\,\bar{\Omega}/\bar{\Omega})^{1/2}$, with $\bar{\Omega} = \alpha_\mathrm{D}\Omega_\mathrm{D} + \alpha_\mathrm{T}\Omega_\mathrm{T}$. The Alfvén velocity is given by $\bar{v}_A = (\Omega_e\bar{\Omega})^{1/2}\,d_e$, where $d_e = c/\omega_{pe}$ is the electron inertial skin depth. In the case of a D–T plasma with equal ion species concentrations, $\alpha_\mathrm{D} = \alpha_\mathrm{T} = \frac{1}{2}$, so that $\bar{\Omega}^2 = \frac{25}{36}\Omega_\mathrm{D}^2$ and $\Omega_{\mathrm{Hy}}^2 = \frac{2}{3}\Omega_\mathrm{D}^2$. The components of the wave-perturbed magnetic field are related through the equations $\tilde{B}_x = i\lambda\tilde{B}_y$ and $k_\parallel\tilde{B}_\parallel = -k_\perp\tilde{B}_y$, with $\tilde{B}_\parallel = -ck_\perp/\omega\tilde{E}_x$.

When the mode frequency ω is above the ion-cyclotron frequency Ω_D (high-frequency range), the dispersion relation simplifies into the magnetohydrodynamic (MHD) dispersion relation $\omega^2 \cong k_\perp^2\bar{v}_A^2$, as shown in Fig. 1.

In this frequency range, the wave polarization is elliptical and the polarization factor λ, which can be rewritten as

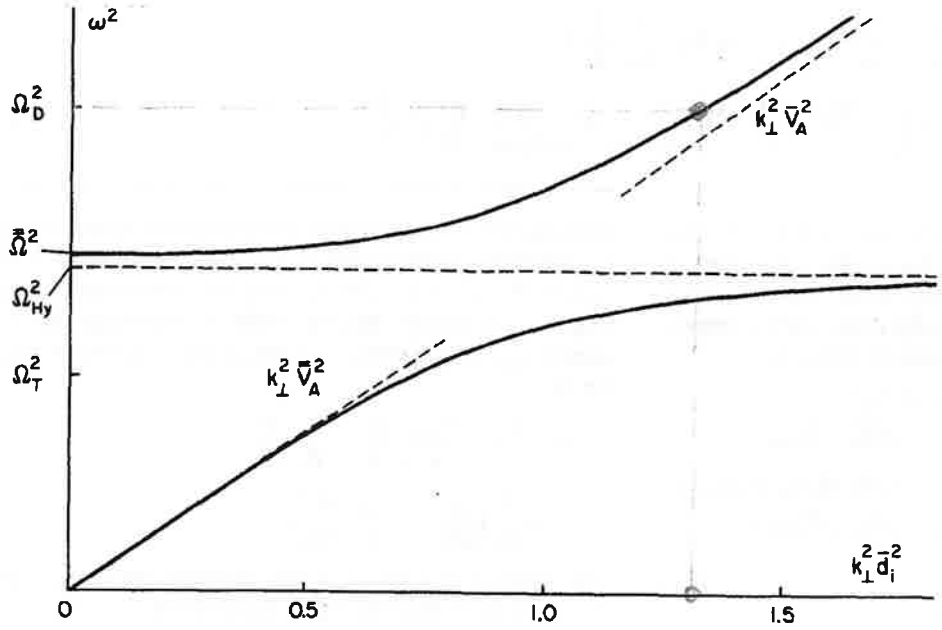

FIG. 1. Graphic representation of the dispersion relation [see Eq. (8)]. The relevant symbols are defined in Sec. II. In particular, $d_i = (m_i/m_e)d_e$ is the ion inertial skin depth and $\bar{v}_A = \bar{v}_A \Omega_{Hy}/\bar{\Omega}$. The two branches correspond to the two "MHD" waves: $\omega^2 \simeq k_\parallel^2 \bar{v}_A^2$ for $\omega > \Omega_D$, and $\omega^2 \simeq k_\perp^2 \bar{v}_A^2$ for $\omega < \Omega_T$.

$\lambda(\omega) = \omega(\alpha_D \Omega_T^2 + \alpha_T \Omega_D^2 - \omega^2)/[\bar{\Omega}(\Omega_{Hy}^2 - \omega^2)]$, scales as $\lambda(\omega) \sim \omega/\bar{\Omega}$. In the low frequency range, $\omega \sim \Omega_D, \Omega_T$, the polarization factor λ varies rapidly from right circular $\lambda = 1$ for $\omega = \Omega_D, \Omega_T$, to left circular $\lambda = -1$ for $\omega = \bar{\Omega}$, to linear, $\lambda = 0$ for $\omega^2 = \alpha_D \Omega_T^2 + \alpha_T \Omega_D^2$ and $\lambda = \infty$ for $\omega = \Omega_{Hy}$. In the frequency interval between Ω_{Hy} and $\bar{\Omega}$, the waves are evanescent with $k^2 = 0$ for $\omega = \bar{\Omega}$ and $k^2 = \infty$ for $\omega = \Omega_{Hy}$.

B. Mode–particle resonances

The resonant interaction between the waves and the high-energy ion population and the damping attributable to the bulk electrons and ions give an imaginary part to the frequency. Setting $\omega = \omega_0 + i\gamma$ with $\gamma \ll \omega_0$, we obtain

$$\gamma = -\mathrm{Re}\,\frac{4\pi\omega^2(1+\lambda^2)}{k^2 c^2}\,\frac{\epsilon^* \cdot \delta\sigma_\perp \cdot \epsilon}{\omega[\partial K(\omega)/\partial\omega]}, \tag{7}$$

where $\epsilon = (1, i\lambda)/(1+\lambda^2)^{1/2}$, $\delta\sigma_\perp$ is the resonant correction to the conductivity tensor and

$$\omega\frac{\partial K}{\partial\omega} = \frac{2\omega^2}{k_\perp^2 \bar{v}_A^2}\,\frac{1 + \Omega_{Hy}^2(\bar{\Omega}^2 - \Omega_{Hy}^2)}{(\omega^2 - \Omega_{Hy}^2)^2} \tag{8}$$

is a positive quantity.

The electron contribution $\delta\sigma_e$ is important when the parallel phase velocity $\omega/k_\parallel$ of the modes is not sufficiently larger than the electron thermal velocity $v_{th\,e}$ and for plasmas with finite values of the ratio $\beta_e = 8\pi n_e T_e/B^2$. The main contribution to $\delta\sigma_e$ [see also Eq. (12)], is given by $\delta\sigma_{xx} = (1/4\pi)(\omega_{pe}^2/\omega)(k_\perp v_{th\,e}/\Omega_e)^2 \zeta_e\, \mathrm{Im}\, Z(\zeta_e)$, where $\zeta_e = \omega/|k_\parallel|\, v_{th\,e}$ and $Z(\zeta_e)$ is the plasma dispersion function. Then the electron damping rate is given by

$$\frac{\gamma_e}{\omega} = -\frac{\pi^{1/2}\beta_e \zeta_e \exp(-\zeta_e^2)}{\omega\,\partial K/\partial\omega}. \tag{9}$$

This damping, usually referred to as transit time damping,[10] is the interaction between the electron magnetic moment μ and the parallel gradient of the mode magnetic field.[11]

The bulk ion contribution $\delta\sigma_D + \delta\sigma_T$ comes from harmonics of the cyclotron resonance of the mode with the ions. Assuming a Maxwellian distribution function for the ions we obtain the damping rate resulting from the i species

$$\frac{\gamma_i^p}{\omega} = -\frac{n_i}{n_e}\,\frac{\pi^{1/2}}{\omega\,\partial K/\partial\omega}\,\frac{\Omega_i\bar{\Omega}}{k_\perp^2 \bar{v}_A^2}\,\frac{\omega}{|k_\parallel| v_{th\,i}}\exp\left(-b_i - \frac{v_{\parallel R}^2}{v_{th\,i}^2}\right)$$
$$\times\left(\frac{b_i}{2}\right)^{p-1}\frac{1}{(p-1)!}\left[p\lambda\left(\frac{\lambda}{2} - 1\right) + p + 1\right] \tag{10}$$

for the resonance with the pth cyclotron harmonic. In Eq. (10) $v_{\parallel R} = (\omega - p\Omega_i)/k_\parallel$, and we have taken the limit $b_i \ll 1$, $b_i = (k_\perp v_{th\,i}/\Omega_i)^2/2$, with $v_{th\,i} = (2T_i/m_i)^{1/2}$ the ion thermal velocity.

Since the density ratio n_h/n_e is small, only the resonant part of $\delta\sigma_h$ need be considered. We calculate the hot-ion perturbed distribution function f_{h1} by including the effects of their density gradient and of their magnetic curvature drift. These effects are outside the homogeneous model but are important in the inhomogeneous analysis in the next section. To include these effects, it will be sufficient to consider a slab model with the equilibrium magnetic field along z, inhomogeneous in the x direction, and with an external force along x simulating the effect of magnetic curvature. The equilibrium distribution function of the hot ions can then be written as $f_{h0} = f_{h0}(\epsilon, \mu, X)$, where $\epsilon = m_h v^2/2$ and $\mu = m_h(\mathbf{v}_\perp - \mathbf{v}_{cdh})^2/(2B_0)$ are the energy and magnetic moment, $\mathbf{v}_{cdh}$ is the magnetic curvature drift velocity, and $X = x + v_y/\Omega_h$ is proportional to the y component of the canonical momentum. Assuming perturbations of the form given in Eq. (1) and using Faraday's equation we obtain from Vlasov equation

$$f_{h1} = -q_h\left\{\frac{i}{\omega\Omega_h m_h}E_{1y}\frac{\partial f_{h0}}{\partial X} - \frac{i}{\omega}(\mathbf{v}_{cdh}\cdot\mathbf{E}_1 + v_\parallel E_{1\parallel})\frac{1}{B_0}\frac{\partial}{\partial\mu}f_{h0}\right.$$
$$\left. + \int_{-\infty}^{t} dt'(\mathbf{E}_1\cdot\mathbf{v}')\left[\frac{\partial}{\partial\epsilon} + \left(1 - \frac{k_\parallel v'_\parallel + \mathbf{k}\cdot\mathbf{v}'_{cdh}}{\omega}\right)\frac{1}{B_0}\frac{\partial}{\partial\mu} + \frac{k_y}{\omega\Omega_h m_h}\frac{\partial}{\partial X}\right]f_{h0}\right\}, \tag{11}$$

where the identity $(i/\omega)(d\mathbf{E}_1/dt) = (1 - \mathbf{k}\cdot\mathbf{v}/\omega)\mathbf{E}_1$ has been used and q_h is the hot-ion charge. The integration in Eq. (11) is performed taking $\rho_h \ll r_n$, where ρ_h is the hot-ion gyroradius and r_n is the characteristic equilibrium density scale length. The resulting conductivity tensor is

$$\delta\sigma_h = iq_h^2\sum_{p=-\infty}^{+\infty}\int d^3v\frac{v_\perp^2(\Pi f_{h0})}{\omega - k_\parallel v_\parallel - p\Omega_h - \omega_{cdh}} \times\begin{pmatrix} J_p'^2(\xi_h) & (ip/\xi_h)J_p(\xi_h)J_p'(\xi_h) \\ -(ip/\xi_h)J_p(\xi_h)J_p'(\xi_h) & (p^2/\xi_h^2)J_p^2(\xi_h)\end{pmatrix}, \tag{12}$$

where the operator Π is defined by

$$\Pi = \frac{\partial}{\partial\epsilon} + \left(1 - \frac{k_\parallel v_\parallel + \omega_{cdh}}{\omega}\right)\frac{1}{B_0}\frac{\partial}{\partial\mu} + \frac{k_y}{m_h\omega\Omega_h}\frac{\partial}{\partial X}, \tag{13}$$

$\omega_{cdh} = k_y v_{cdh}$ is the magnetic curvature drift frequency, and $J_p(\xi_h)$ and $J_p'(\xi_h) \equiv dJ_p(\xi_h)/d\xi_h$ are Bessel functions of argument $\xi_h = k_\perp v_\perp/\Omega_h$. Taking the resonant part of $\delta\sigma_h$ in Eq. (12) we obtain the hot-ion contribution to γ

$$\gamma_h = \frac{n_h}{n_e}\frac{\omega^2}{\omega\,\partial K/\partial\omega}\frac{\Omega_h\bar{\Omega}}{k_\parallel^2\bar{v}_A^2}\pi \times\sum_{p=-\infty}^{+\infty}\left(\frac{p\Omega_h}{k_\perp v_h}\right)^2\int d^3v\,\delta(\omega - k_\parallel v_\parallel - p\Omega_h - \omega_{cdh}) \times\frac{2\epsilon_h}{n_h}\left(\lambda J_p(\xi_h) - \frac{\xi_h}{p}J_p'(\xi_h)\right)^2\Pi f_{h0}. \tag{14}$$

All coefficients in Eq. (14) multiplying Πf_{h0} are positive definite. In the homogeneous case, the operator Π reduces to $\partial/\partial\epsilon + B_0^{-1}\partial/\partial\mu \equiv (2/m_h)\partial/\partial v_\parallel^2$, and the portion of velocity space where $\Pi f_{h0} > 0$ (instability region) gives a positive contribution to γ_h. Positive values of $\partial f_{h0}/\partial v_\parallel^2$ can occur either for isotropic but nonmonotonic distribution functions, or for anisotropic distribution functions with a positive slope in the perpendicular direction. A positive growth rate γ_h will result if the parameters ω and $k_\parallel$ can be chosen such that, roughly speaking, the resonant surface lies mainly inside the instability region. For each cyclotron harmonic, the shape of the p resonant surface is determined by the resonance condition expressed in the δ function of Eq. (14). The magnetic curvature drift frequency depends on ϵ,μ through the combination $\epsilon - \mu/(2B_0)$. Thus, the resonant surfaces in velocity space are given by ellipsoids $(v_\parallel - v_s)^2 + v_\perp^2/2 = \text{const}$, with $v_s = k_\parallel\epsilon_h/(m_h\omega_{cdh}^0)$ and $\omega_{cdh}^0 = \omega_{cdh}$ $(\epsilon = \epsilon_h, \mu = 0)$. If $\omega_{cdh}^0 \gg k_\parallel v_h$, the center of the ellipsoids approaches the origin in velocity space. In the opposite limit, the resonant surfaces reduce to a plane $v_\parallel = \text{const}$.

In the inhomogeneous slab model, assuming that only the density of the high-energy ion population depends on x, f_{h0} contains a spatial factor that can be written as $(1 - x/r_{nh})$, with $r_{nh}^{-1} = (-d\ln n_h/dx)$ the characteristic scale length of the hot ion density. Defining a diamagnetic frequency $\omega_{*h} = k_y v_h^2/(\Omega_h r_{nh})$, the operator Π can be written as

$$\Pi = \left(1 - \frac{\omega_{*h}}{\omega}\right)\frac{\partial}{\partial\epsilon} + \frac{1}{B_0}\frac{\partial}{\partial\mu} \equiv \frac{2}{m_h}\left(\frac{\partial}{\partial v_\perp^2} - \frac{\omega_{*h}}{\omega}\frac{\partial}{\partial v_\parallel^2}\right).$$

The presence of a strong density gradient (small r_{nh}) can then alter the instability region significantly.

III. NORMAL MODES IN AN INHOMOGENEOUS PLASMA CONFIGURATION

The ratio γ_h/ω derived in the previous section scales as n_h/n_e, which is, by hypothesis, a small quantity. The rate at which energy is transferred to the modes from the high-energy ion population is therefore slow. Thus, in addition to considering the changes introduced in the resonant responses of the bulk species and the hot ions by the plasma inhomogeneity, we must ascertain whether the modes of interest exist as normal modes in a realistic plasma configuration. In fact, a relatively small rate of spatial convection could be sufficient to drain away the energy gained through the resonant interaction and stabilize the modes.

In order to deal with problems of increasing complexity in constructing the relevant eigenmodes, we shall first consider a simplified inhomogeneous model that can be viewed as referring to a torus of large aspect ratio and vanishing poloidal field. On the basis of the information obtained from this model, we shall later derive the full dispersion equation for a realistic toroidal configuration and solve it in the high-frequency range, i.e., when $\omega^2 \gg \Omega_{Hy}^2, \bar{\Omega}^2$, by means of a combined expansion in inverse powers of the poloidal number and of the aspect ratio.

A. Localized modes

Referring to polar coordinates in the poloidal plane, we consider the perturbed parallel magnetic field, which we take in the form $B_{1\parallel} = \tilde{B}(r,\theta)\exp[-i(\omega t - k_\parallel z)]$, as the appropriate physical variable.

Then we write the differential form of the dispersion relation $\omega^2 = k^2\bar{v}_A^2$ heuristically as

$$\frac{1}{r}\frac{\partial}{\partial r}r\frac{\partial}{\partial r}\tilde{B} + \frac{1}{r^2}\frac{\partial^2}{\partial\theta^2}\tilde{B} = -\frac{\omega^2}{\bar{v}_{A0}^2}\frac{n(r)}{n_0}\frac{(B_0^0)^2}{B_0^2(r,\theta)}\tilde{B}, \tag{15}$$

where $\bar{v}_{A0}$, n_0, and B_0^0 are the Alfvén velocity, plasma density, and magnetic field at the magnetic axis. We take

JET Experiments [4]

* No significant indication of interaction between a $\omega = \Omega_T$ mode and the electron population
* Evidence for interactions [5] involving the electron population that could be described by $(\text{as } \Omega_\alpha = \Omega_D)$

$$p^0 \Omega_\alpha = k_\parallel V_\parallel^e - \Omega_e$$

with $p^0 =$ integer and $V_\parallel^e >> V_{the}$.

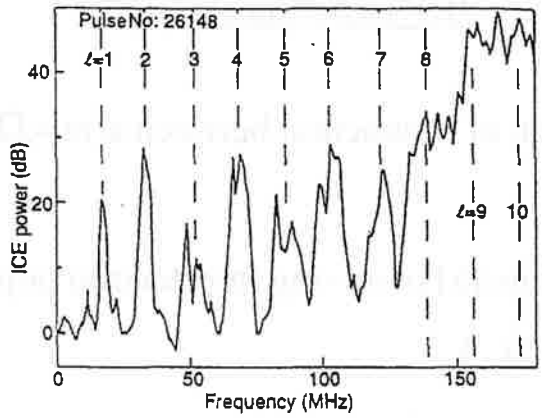

Fig. 1. Emission at the harmonics of the ^{4}He cyclotron frequency measured in a D–T plasma near the time where the neutron emission is peaking (fig. reproduced from ref. [2]).

References

[1] B. Coppi, S. Cowley, R. Kulsrud, P. Detragiache and F. Pegoraro, Phys. Fluids 12 (1986) 4060.

[2] G.A. Cottrell, V.P. Bhatnagar, O. da Costa, R.O. Dendy, A. Edwards, J. Jacquinot, M.F.F. Nave, M. Schmid, A. Sibley, P. Smeulders and D.F.H. Start, in: Proc. 1992 Plasma Physics Conf. of the European Physical Society, Innsbruck (1992), to be published.

[3] JET Team, Nucl. Fusion 32 (1992) 193.

[4] B. Coppi, M.N. Rosenbluth and R.N. Sudan, Ann. Phys. 55 (1969) 207.

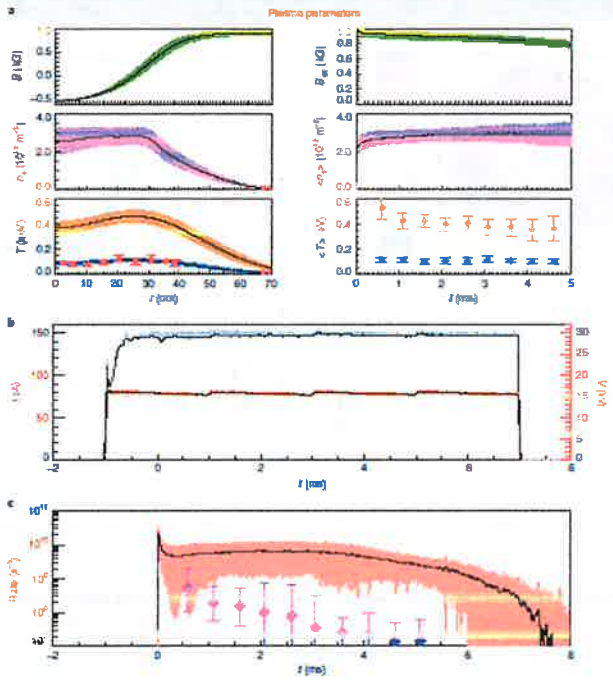

Fig. 2 | Basic plasma and N01 parameters, and a comparison of the measured and calculated neutron emission rates. a, Radial profiles (left column, taken at $t = 1.5$ ms)) and time histories (right column) of plasma parameters averaged over 57 similar shots. Top row: rigid rotor magnetic field profile (note that the internal magnetic field is not measured) and external magnetic field as a function of time. Middle row: Abel-inverted electron density and the time history of the average density inside the FRC. Bottom row: electron temperature profile measured by Thomson scattering (red diamonds), by an edge Langmuir probe (red triangles) and the interpolated profile used in the fusion rate calculation (black line with blue error bars). The upper limit ion temperature profile is shown with orange error bars. The right panel shows the time history of the temperatures at the field null, with ions in orange and electrons in blue. **b**, N01 counters (black line with cyan error bars, left axis) and voltage (red, right axis), both averaged over the five beams. **c**, Measured neutron rate (black line with salmon error bars) and calculated thermonuclear fusion rate (purple diamonds). In all cases, error bars represent s.d. of the mean.

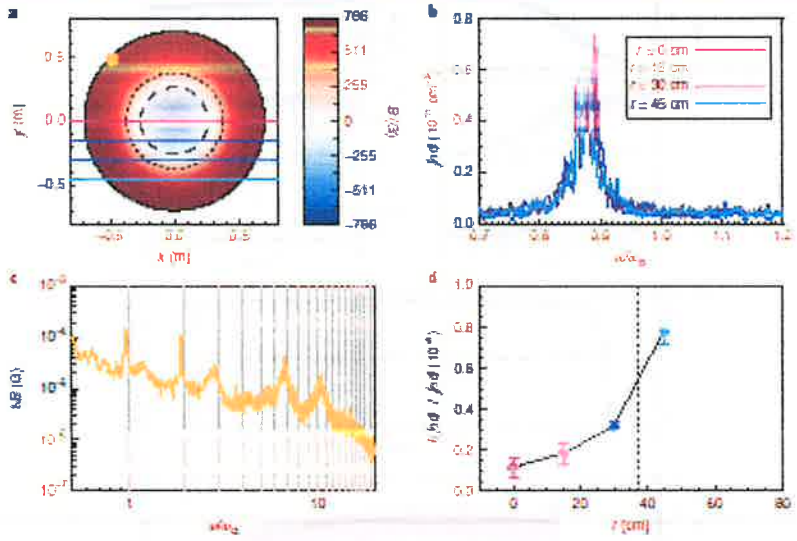

Fig. 3 | Summary of measurements of fluctuations in the electron density and magnetic field associated with the beam-driven mode. a, An ideal magnetic equilibrium shows the magnetic field strength (colour map), separatrix (dotted line) and field null (dashed line), as well as the measurement locations of the density (coloured horizontal lines) and magnetic field (orange dot). **b**, Density fluctuation spectra show a clear peak near the ion cyclotron frequency ω_{ci} at all radii, even those outside the separatrix. **c**, Magnetic fluctuation spectrum, showing that multiple harmonics of ω_{ci} are excited. **d**, Size of the density fluctuations relative to the mean density peaks outside the separatrix. Error bars are propagated from the s.d. of the time-averaged line-integrated density and the 1σ error estimate of a Gaussian fit to the frequency spectrum.

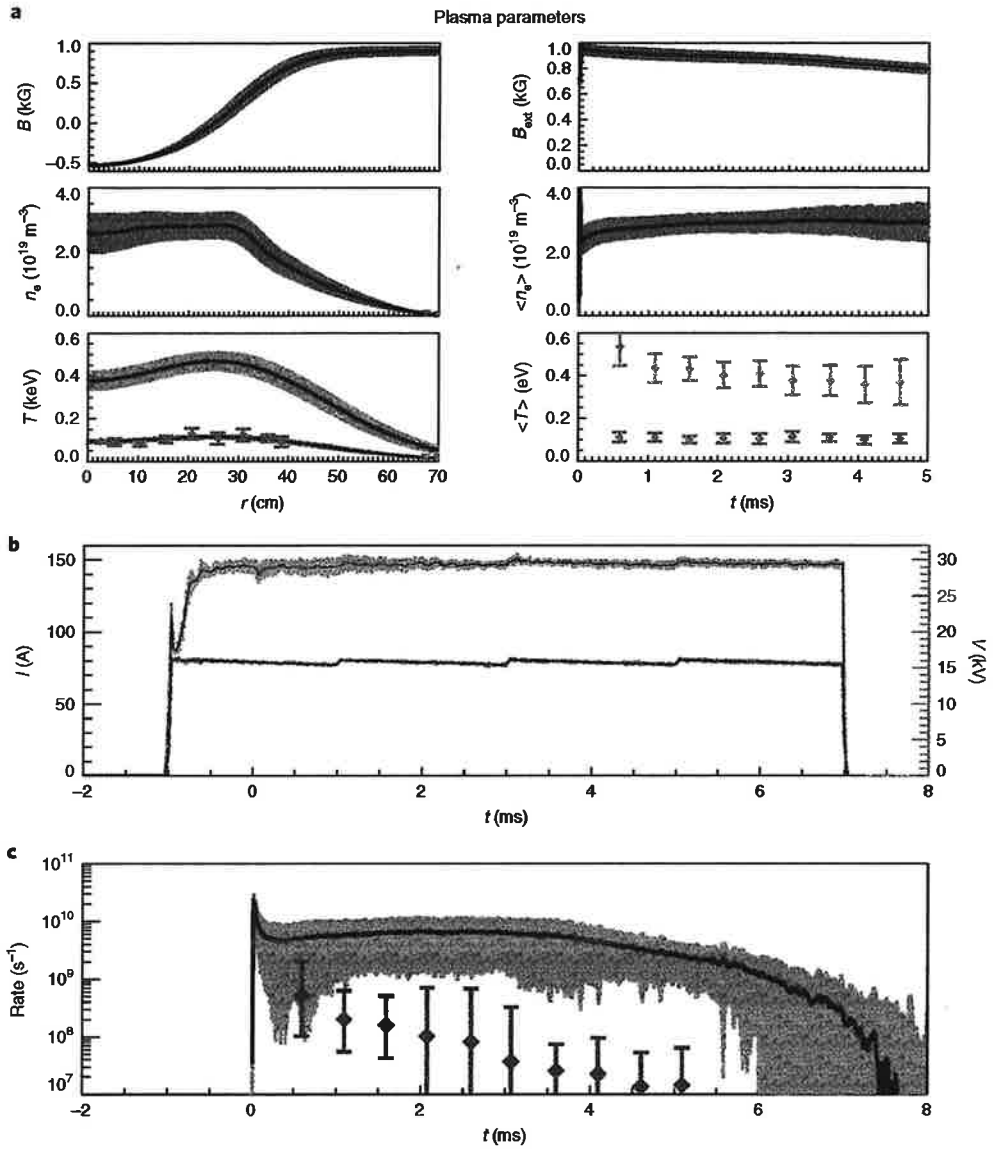

Fig. 2 | Basic plasma and NBI parameters, and a comparison of the measured and calculated neutron emission rates. a, Radial profiles (left column, taken at $t=1.5$ ms)) and time histories (right column) of plasma parameters averaged over 57 similar shots. Top row: rigid rotor magnetic field profile (note that the internal magnetic field is not measured) and external magnetic field as a function of time. Middle row: Abel-inverted electron density and the time history of the average density inside the FRC. Bottom row: electron temperature profile measured by Thomson scattering (red diamonds), by an edge Langmuir probe (red triangles) and the interpolated profile used in the fusion rate calculation (black line with blue error bars). The upper limit ion temperature profile is shown with orange error bars. The right panel shows the time history of the temperatures at the field null, with ions in orange and electrons in blue. **b**, NBI current (black line with cyan error bars, left axis) and voltage (red line, right axis), both averaged over the five beams. **c**, Measured neutron rate (black line with salmon error bars) and calculated thermonuclear fusion rate (purple diamonds). In all cases, error bars represent s.d. of the mean.

wave. This mode propagates nearly perpendicularly to the magnetic field at harmonics of the ion cyclotron frequency.

The ion velocity distribution output from the mirror plasma simulation is shown in Fig. 5b. As the simulation evolves, the modes grow and one can see a high-energy tail drawn out from the main ion energy distribution in a time much shorter than the beam slowing down time. This tail is small enough to have a negligible effect on the macroscopic distribution (that is, the temperature as determined by a Gaussian fit does not change, as illustrated by the solid lines), but large enough to have a significant impact on the fusion reactivity, due to the sensitive dependence of the fusion cross-section on particle energy. Figure 5c shows the fusion rate calculated by numerically summing over binary collisions. It can be seen that in 8 μs, less than 1/100th of a beam slowing down time, the fusion reaction rate is increased by a factor of 30 above thermonuclear.

Based on the high-energy tail and enhanced fusion observed in this simulation, we conclude that the beam-driven mode is probably more active in the mirror plasma than in the core. This localization may also explain why the fluctuations do not degrade confinement of the FRC core.

A simple criterion based on Wakefield theory[22] can be used to estimate the size of the wave electric field of the saturated ion Bernstein mode. In Wakefield theory, the mode amplitude saturates at the Tajima–Dawson field, $E=m_e c\omega_p/e$, where m_e is the electron mass, c is the speed of light, ω_p is the plasma frequency and e is the electron charge. Simply put, the maximum velocity a

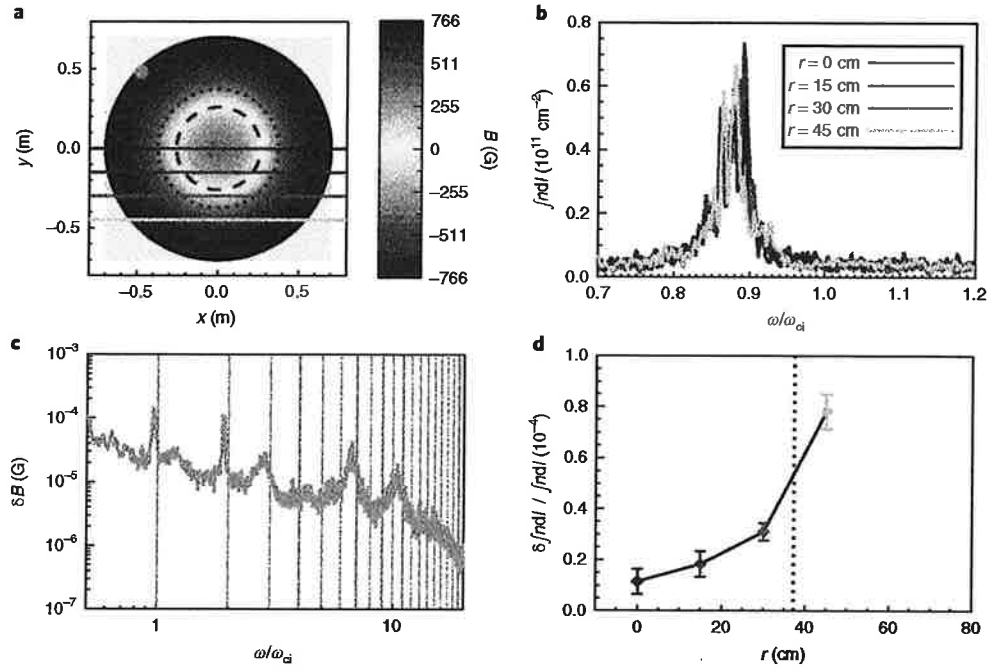

Fig. 3 | Summary of measurements of fluctuations in the electron density and magnetic field associated with the beam-driven mode. a, An ideal magnetic equilibrium shows the magnetic field strength (colour map), separatrix (dotted line) and field null (dashed line), as well as the measurement locations of the density (coloured horizontal lines) and magnetic field (orange dot). **b**, Density fluctuation spectra show a clear peak near the ion cyclotron frequency, ω_{ci}, at all radii, even those outside the separatrix. **c**, Magnetic fluctuation spectrum, showing that multiple harmonics of ω_{ci} are excited. **d**, Size of the density fluctuations relative to the mean density peaks outside the separatrix. Error bars are propagated from the s.d. of the time-averaged line-integrated density and the 1σ error estimate of a Gaussian fit to the frequency spectrum.

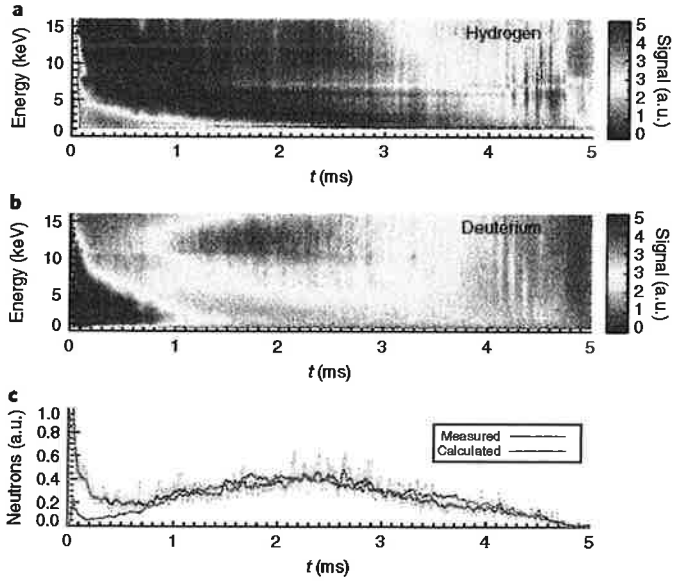

Fig. 4 | Measurements of the energy spectra of charge exchange neutrals at the edge of the plasma reveal ion acceleration coincident with a rise in neutron emission. a–c, Neutral hydrogen (beam species) energy spectrum (**a**), neutral deuterium (plasma species) energy spectrum (**b**) and measured (blue with grey error bars representing s.d. of the mean) and calculated (red) neutron flux (**c**). The calculated neutron flux is obtained from the measured deuterium energy spectrum.

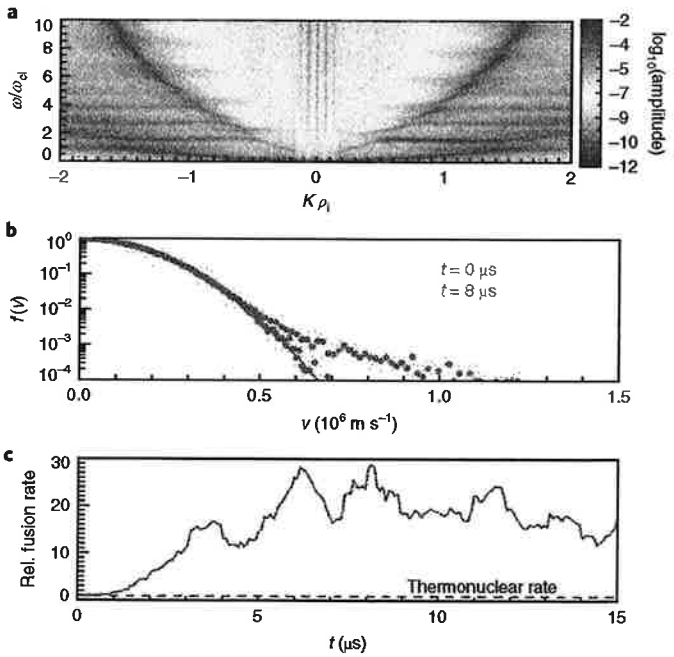

Fig. 5 | Simulation of the beam-plasma system reveals the three features observed in experiment: fluctuations at harmonics of the ion cyclotron frequency, a high-energy tail on the main ion species and enhanced neutron production. a, Dispersion relation from PIC simulation of $\beta = 0.1$ plasma showing the excitation of multiple ion Bernstein modes at harmonics of the ion cyclotron frequency. **b**, Plasma ion velocity distributions at $t = 0$ (blue) and $t = 8\,\mu s$ (red) in the simulation. The Gaussian fits for each time are plotted as solid lines and overlay each other. **c**, Corresponding neutron rate, normalized to the thermonuclear rate, as a function of time. The generated tail enhances the fusion rate by a factor of nearly 30.

particle can obtain from electric field acceleration in a wave period is the phase velocity. By making the substitutions $m_e \rightarrow M$, $c \rightarrow v_\phi$ and $\omega_p \rightarrow \omega_{ci}$ we obtain the ion Bernstein analogue, $E_{sat} = Mv_\phi\omega_{ci}/e$, where M is the deuteron mass, v_ϕ is the wave phase velocity and

NON-THERMAL FISION BURNING PROCESSES, RELEVANT COLLECTIVE MODES AND GAINED PERSPECTIVES

B. COPPI
Massachusetts Institute of Technology and CNR
Cambridge, USA and Rome, Italy
Email: coppi@mit.edu

B. BASU
Massachusetts Institute of Technology
Cambridge, USA

Abstract

New tridimensional plasma structures, that are oscillatory and classified as non-separable ballooning modes, can emerge in inhomogeneous plasmas and undergo resonant mode-particle interactions, e.g., with a minority population, that can lead them to modify their spatial profiles. Thus, unlike the case of previously known ballooning modes their amplitudes are not separable functions of time and space. The relevant resonance conditions are intrinsically different from those of the well-known Landau conditions for (ordinary) plasma waves: they involve the mode geometry and affect different regions of the distribution in momentum space at different positions in configuration space. A process for a transfer of energy among different particle populations is envisioned.

1. INTRODUCTION

The same factors that make the physics of magnetically confined fusion burning plasmas difficult to predict provide also the opportunity to identify novel processes extending the range of meaningful fusion burn conditions which can be achieved beyond those predicted on the basis of (conventional) thermonuclear fusion theory.

In fact, weakly collisional and well confined plasmas have been found to be strongly influenced by the presence of collective modes and self-organization processes [1]. In fusion burning regimes, where the plasma energy is supplied by the charged reaction products, self-organization is expected to be more important than in present and past experiments where plasma heating is provided by an external and controlled source. Then new modes or new forms of previously known modes can be expected to emerge. In particular, given the relevance of novel [2] resonant mode-particle interactions [3], it is reasonable to expect that the distributions of the reacting nuclei in momentum space will not remain strictly Maxwellian and that the resulting reaction rates will be different from those evaluated for (conventional) thermalized plasmas.

The present paper is organized as follows; In Section 2, the topology of non-separable ballooning modes [4,5] that can be excited in an axisymmetric confinement configuration is described as geometry plays a key role in the processes identified in later sections. In Section 3, the magnetosonic modes found for multispecies homogeneous plasmas are introduced in order to identify the range of plasma parameters for which the theory of modes emerging in inhomogeneous deuterium – tritium plasmas is developed. In Section 4, the class of mode-particle resonant interactions that are involved in the transfer of energy from the α - particle population to the deuterons are identified. In Section 5, the analysis showing that the considered ballooning modes are localized radially, and their energy is contained, is given. In Section 6, the ballooning profile along magnetic field lines of the considered modes is derived in the absence of mode-particle interactions and, in addition, the (novel) conditions for these interactions are introduced and shown to be intrinsically different from those considered in Section 4, referring to "ordinary" waves. In Section 7, the intrinsically different time and space dependence of the mode amplitude and profile, from that of well-known waves, resulting from resonant interactions with a minority particle population is demonstrated. In Section 8, the amplitudes of the plasma density fluctuations associated with realistic rates of energy extraction from the emitted α - particle population are estimated. In Section 9, results from two different sets of experiments are discussed which lend support to the presented theory. In Section 10, final considerations based on the presented theory are made.

2. NON-SEPARABLE HIGH FREQUENCY MODES

We refer, for simplicity, to a toroidal plasma with a large aspect ratio, a circular cross section and high toroidal and poloidal magnetic fields, the former being represented by $B \simeq B_0 / \left(1 + r\cos\theta / R_0\right)$ where R_0 is the major radius, r the (minor) radial coordinate and θ the poloidal angle. Moreover, the assumed poloidal field $B_\theta \simeq B_\theta\left(r\right)$ is smaller than B_0, that is $B_\theta^2 / B_0^2 << 1$, and $\left|dB_\theta / dr\right| / \left|B_\theta\right| \sim \left|dn / dr\right| / n \sim 1/a$, a being the torus minor radius. The transverse plasma pressure $p_\perp = \left(p_e + p_D + p_T\right)_\perp$ is taken to be $<< B_0^2 / 8\pi$. Then, to lowest order in the small considered parameters, the radial equilibrium condition reduces to

$$0 = -\frac{\partial}{\partial r}\left(p_e + p_i\right)_\perp - \frac{1}{c}\left(J_\varphi B_\theta - J_\theta B_\varphi\right). \tag{1}$$

The ballooning modes [4,5] that are introduced for this configuration are represented by plasma density perturbations of the form

$$\hat{n} = \tilde{n}\left(\theta, r - r_0^0, t\right)\exp\left(-i\omega t - im^0\theta + in^0\varphi\right), \tag{2}$$

where m^0 and n^0 are integers,

$$\left|\omega\right| >> \frac{1}{\tilde{n}}\frac{\partial\tilde{n}}{\partial t}, \tag{3}$$

$$\left|\frac{m^0}{r_0^0}\right| > \left|\frac{1}{\tilde{n}}\frac{\partial\tilde{n}}{\partial r}\right|, \tag{4}$$

$\tilde{n}\left(\theta, r - r_0^0, t\right)$ is a non-separable function of t, θ, $r - r_0^0$ which is periodic in θ and is radially localized around the surface $r = r_0^0$, that is with $\left|\left(\partial\tilde{n} / \partial r\right) / \tilde{n}\right| > 1/a$ where a is the plasma minor radius. Clearly, we are concerned with a special class of ballooning modes. We may then adopt the "disconnected mode" approximation [5], for $\left|\theta\right| < \pi$, and reduce $\hat{n}$ to be represented by

$$\hat{n} \simeq \tilde{n}\left(\theta, t\right)G\left(r - r_0^0\right)\exp\left\{-i\omega t + in^0\left[\varphi - q\left(r - r_0\right)\theta\right]\right\}, \tag{5}$$

where $q\left(r\right) \simeq B_0 r / \left[R_0 B_\theta\left(r\right)\right]$, $q\left(r = r_0\right) = m^0 / n^0 \equiv q_0$ and $\left|r_0 / r_0^0 - 1\right| < r_0 / R_0$. Then

$$\mathbf{B}\cdot\nabla\hat{n} \simeq \frac{B_0}{q_0 R_0}\frac{\partial\tilde{n}}{\partial\theta}G\left(r - r_0^0\right)\exp\left\{-i\omega t + in^0\left[\varphi - q\left(r - r_0\right)\theta\right]\right\}. \tag{6}$$

In particular, we consider $\tilde{n} = \tilde{n}_{\text{ev}} + \tilde{n}_{\text{od}}$ where $\tilde{n}_{\text{ev}}$ and $\tilde{n}_{\text{od}}$ are even and odd functions of θ, respectively, $\left|\tilde{n}_{\text{ev}}\left(\theta = \pi\right) / \tilde{n}_{\text{ev}}\left(\theta = 0\right)\right| << 1$, as required for the validity of the disconnected mode approximation, and the component $\tilde{n}_{\text{od}}$ is not involved in the cold, homogeneous plasma approximation [6].

3. MULTISPECIES MAGNETOSONIC MODES

The modes that, for an infinite, homogeneous and cold plasma correspond to those under consideration can be classified as multispecies magnetosonic modes [6]. These are represented by $\hat{n} = \tilde{n}_k \exp\left(-i\omega t + ik_\perp y + ik_\parallel z\right)$, where $k_\perp$ corresponds to m^0 / r_0. If we adopt the "disconnected

mode" approximation represented by Eq. (5), and refer to Eq. (6), $ik_{\|}\tilde{n}_k$ can simulate $\left[1/\left(qR_0\right)\right]\left(\partial\tilde{n}/\partial\theta\right)$.

Since the modes of interest are those that can extract energy [3] from the α - particle population produced by the DT fusion reaction, the most appropriate frequency to consider is

$$\omega \simeq \frac{m^0}{r_0}\bar{\mathrm{V}}_A = \Omega_\alpha + \delta\omega, \tag{7}$$

where $\bar{\mathrm{V}}_A^2 = \left[B^2/\left(4\pi n_e m_D\right)\right]\left(n_D + 2n_T/3\right)/n_e$, Ω_α is the α - particle cyclotron frequency and $\left|\delta\omega\right| < \Omega_\alpha$. Referring to the dispersion relation presented in Ref. [3], condition (7) corresponds to

$$m^0 \simeq r_0\omega_{pD}/c \equiv r_0/d_D >> 1$$

where $\omega_{pD}^2 = 4\pi n_D e^2/m_D$, $d_D = c/\omega_{pD}$, n_e, n_D and n_T are the densities of the electron, deuteron and triton populations. In fact, the cold homogeneous plasma dispersion relation {Eq. (6) in Ref. [3]} is

$$\frac{\omega^2 - \bar{\bar{\Omega}}^2}{\omega^2 - \Omega_{Hy}^2}\omega^2 = \left(k_\perp^2 + k_{\|}^2\right)\bar{\mathrm{V}}_A^2, \tag{8}$$

where $\bar{\bar{\Omega}} = \left(n_D\Omega_T + n_T\Omega_D\right)/n$, $\Omega_{Hy}^2 = \Omega_D\Omega_T\left(\bar{\bar{\Omega}}/\bar{\Omega}\right)$ and $\bar{\Omega} = \left(n_D\Omega_D + n_T\Omega_T\right)/n$. We can verify that for $\omega \simeq \Omega_D \simeq 5\times10^8\left(B/10\ T\right)rad/s$, and $n_D = n_T = n/2$, ω^2 is close to $\left(k_\perp^2 + k_{\|}^2\right)\bar{\mathrm{V}}_A^2$.

4. "CONVENTIONAL" MODE-PARTICLE RESONANT INTERACTIONS

Referring, for simplicity, to the homogeneous model, we note that the mode-particle resonance $\omega - \Omega_\alpha + k_{\|}\,\mathrm{v}_{\|}\big)_\alpha = 0$ is involved in extracting energy [3] from the α - particle population. For this, significant values of $k_\perp\rho_\alpha$ have to be considered [1], where $\rho_\alpha = \mathrm{V}_\alpha/\Omega_\alpha$, V_α being the velocity of the emitted α - particles. We note that, considering $n_T \simeq n_D$, the value of $k_\perp d_D$ is the main parameter that identifies the relevant limits of the dispersion relation. The ratio $\rho_\alpha/d_D = \mathrm{V}_\alpha/\mathrm{V}_{AD}$ is computed where $\mathrm{V}_{AD}^2 = B^2/\left(4\pi m_D n_D\right)$. In particular, $k_\perp\rho_\alpha \simeq \left(3.5n_D/10^{21}m^{-3}\right)^{1/2}\left(10\ T/B\right)k_\perp d_D$ and $k_\perp d_D \sim 1$ can correspond to significant value of $k_\perp\rho_\alpha$ for attainable plasma confinement parameters. Clearly, when referring to the ballooning modes represented by Eq. (5) m^0/r_0 corresponds to $k_\perp$.

Referring to the energy absorbing resonance $\omega - \Omega_D + k_{\|}\,\mathrm{v}_{\|}\big)_D = 0$ we notice that $k_{\|}\mathrm{v}_{\|}\big)_D \simeq k_{\|}\mathrm{v}_{\|}\big)_\alpha$ and the needed two resonances with the two populations will have to involve different $k_{\|}$'s. Moreover, mode particle resonant interactions with the main body of the electron distribution, transferring considerable energy to it, are avoided as $\bar{\omega}_{te} << \Omega_\alpha << \Omega_e$ where $\bar{\omega}_{te}$ is the average electron transit frequency. On the other hand, the transfer of energy to the tail of the electron distribution corresponding to $\Omega_\alpha = k_{\|}\mathrm{v}_{\|}\big)_e$ should be considered as a plasma diagnostic means [8]

involving the emission of e.m. radiation at the frequency $\omega = \Omega_\alpha$. This has been, in fact, observed by the DT plasma experiments reported in Ref. [9]. Moreover, since finite values of $k_\perp \rho_\alpha$ are involved, higher harmonic modes can be excited as well. In the case of the deuterons we have to consider that, correspondingly, $\left(k_\perp \rho_D\right)^2 << 1$.

5. RADIAL CONTAINMENT

The radial localization of the modes we are considering is like that of the waves which were proposed [9] as being responsible for the experimentally observed e. m. emission at the harmonics of α - cyclotron frequency. The radial containment of a mode can, in fact, be viewed as a positive characteristic in view of preventing loss of its energy toward surrounding walls.

As indicated in the previous section we choose to consider mode spatial profiles represented by $\tilde{n}\left(r - r_0, \theta\right) = \tilde{\tilde{g}}\left(r - r_0^0\right) \tilde{\tilde{f}}\left(\theta, r_0^0\right)$. In order to evaluate $\tilde{\tilde{g}}\left(r - r_0^0\right)$ we neglect the effects of toroidicity that are included in $\tilde{\tilde{f}}\left(\theta, r_0^0\right)$. We refer to modes with frequencies $\omega \simeq m^0 \mathrm{V}_A^0 / r_0$ where $\mathrm{V}_A^0 = B / \left[4\pi\rho\left(r_0\right)\right]^{1/2}$, $\rho = \bar{m}_i n\left(r\right) = m_D n_D + m_T n_T$, and $\left(m^0\right)^2 >> 1$.

Then, adopting the ideal MHD approximation and following a standard procedure {see Ref. [8]}, based on the same equations considered in Section 6, we are led to find the following equation for $\tilde{\tilde{g}}\left(r - r_0^0\right)$

$$\frac{d^2 \tilde{\tilde{g}}}{dr^2} - \left[\frac{\left(m^0\right)^2}{r^2} - \frac{\omega^2}{\left(\mathrm{V}_A^0\right)^2} \frac{n\left(r\right)}{n_0}\right] \tilde{\tilde{g}} = 0 \tag{9}$$

where n_0 is the peak particle density and $\left(\mathrm{V}_A^0\right)^2 = B^2 / \left(4\pi n_0 m_i\right)$. Then $\omega_0^2 / \left(m^0\right)^2$ can be chosen in such a way that r_0^0 defined by

$$\frac{\left(m^0\right)^2 \left(\mathrm{V}_{A0}^0\right)^2}{r_0^0 \omega_0^2} = 1, \tag{10}$$

for $\left(\mathrm{V}_{A0}^0\right)^2 = B^2 / \left[4\pi m_i n\left(r = r_0^0\right)\right]$, and by

$$2\frac{\left(m^0\right)^2}{\left(r_0^0\right)^3} + \frac{\omega_0^2}{\left(\mathrm{V}_{A0}^0\right)^2} \left(\frac{1}{n}\frac{dn}{dr}\right)_{r=r_0^0} = 0 \tag{11}$$

falls within the plasma column. In fact, Eqs. (10) and (11) imply that

$$\left(\frac{1}{n}\frac{dn}{dr}\right)_{r=r_0^0} = -\frac{2}{r_0^0}. \tag{12}$$

Consequently, Eq. (9) reduces to

$$\frac{d^2\tilde{\tilde{g}}}{dr^2}-\left\{\left[\frac{6\left(m^0\right)^2}{\left(r_0^0\right)^4}-\frac{\omega_0^2}{\left(\mathrm{V}_A^0\right)^2}\frac{1}{n_0}\frac{d^2n}{dr^2}\right]\frac{1}{2}\left(r-r_0^0\right)^2-\frac{\left(\delta\omega_1^2\right)}{\left(\mathrm{V}_A^0\right)^2}\frac{n\left(r_0^0\right)}{n_0}\right\}\tilde{\tilde{g}}=0 \tag{13}$$

for $\omega^2\simeq\omega_0^2+\left(\delta\omega^2\right)_1$. The relevant solution is

$$\tilde{\tilde{g}}=\tilde{\tilde{g}}_0\exp\left[-\frac{1}{2}\frac{\left(r-r_0^0\right)^2}{\Delta_r^2}\right] \tag{14}$$

where

$$\Delta_r^4=\frac{\left(r_0^0\right)^4}{3\left(m^0\right)^2}\Big/\left[1-\frac{\left(r_0^0\right)^2}{6}\left(\frac{1}{n}\frac{d^2n}{dr^2}\right)_{r=r_0^0}\right]<<a^4, \tag{15}$$

a is the plasma minor radius and

$$\left(\delta\omega^2\right)_1\simeq\omega_0^2\Delta_r^2\left(\frac{1}{n}\frac{dn}{dr}\right)_{r=r_0^0}. \tag{16}$$

In particular,

$$\frac{\left(\delta\omega^2\right)_1}{\omega_0^2}=\left(\frac{r_0^0}{m^0\Delta_r}\right)^2$$

implies that $\left(m^0\right)^2>\left(r_0^0/\Delta_r\right)^2$ as assumed. As an example, we note that if $n\simeq n_0\left(1-r^2/a^2\right)$, condition corresponds to $r_0^0=a/\sqrt{2}$.

6. INITIAL BALLOONING MODE PROFILE

The derivation of the ballooning mode equation is greatly simplified by the observation made in Section 3 that modes with $\omega\simeq\Omega_D$ and $kd_D\sim1$ can be described by the relatively simple theory of magnetosonic modes where both deuterons and tritons can be treated in the limit $\omega^2>\Omega_D^2$. Then the particle conservation equation

$$-i\omega\hat{n}+n\nabla\cdot\hat{\mathbf{u}}_e\simeq0 \tag{17}$$

is combined with the total momentum conservation equation

$$-i\omega\left(m_Dn_D\hat{\mathbf{u}}_D+m_Tn_T\hat{\mathbf{u}}_T\right)=-\nabla\left(\hat{p}_e+\hat{p}_i+\frac{\hat{\mathbf{B}}\cdot\mathbf{B}}{4\pi}\right)+\frac{1}{4\pi}\left(\mathbf{B}\cdot\nabla\hat{\mathbf{B}}+\hat{\mathbf{B}}\cdot\nabla\mathbf{B}\right) \tag{18}$$

where the contribution of the α - particle population, considered a minority species, is not included and $\hat{n}=\hat{n}_D+\hat{n}_T=\hat{n}_e$.

Referring to the toroidal configuration introduced in Section 2, we take $B\simeq B_m+\Delta B$, where B_m is the minimum field corresponding to $\theta=0$, $B_m\simeq B_0\left(1-r/R_0\right)$. Then $\Delta B/B_0\simeq\left(r/R_0\right)\left(1-\cos\theta\right)$. The equation $\hat{\mathbf{E}}+\hat{\mathbf{u}}_e\times\mathbf{B}/c=0$ combined with $-\partial\hat{\mathbf{B}}/\partial t=c\nabla\times\hat{\mathbf{E}}$ leads to

$$-i\omega\hat{\mathbf{B}} = \mathbf{B}\cdot\nabla\hat{\mathbf{u}}_e - \mathbf{B}\left(\nabla\cdot\hat{\mathbf{u}}_e\right) \tag{19}$$

that is

$$-i\omega\hat{B} = B\left(\nabla_{\|}\hat{u}_{e\|} - \nabla\cdot\hat{\mathbf{u}}_e\right),$$

where $\nabla_{\|} = \left(\mathbf{B}/B\right)\cdot\nabla$, and

$$\frac{\hat{B}}{B} = -\frac{i}{\omega}\left(\nabla\cdot\hat{\mathbf{u}}_e - \nabla_{\|}\hat{u}_{e\|}\right). \tag{20}$$

Therefore,

$$\frac{\hat{B}}{B} = \frac{\hat{n}}{n} + \frac{i}{\omega}\left(\nabla_{\|}\hat{u}_{e\|}\right). \tag{21}$$

Next, considering that $\beta \equiv 8\pi\left(p_e + p_i\right)/B^2 << 1$ we take $\left|\hat{p}_e\right| \sim \left|\hat{p}_i\right| << \left|\hat{\mathbf{B}}\cdot\mathbf{B}/4\pi\right|$ and, for $\hat{\rho} = \hat{n}m_D\left(n_D + m_D n_T/m_T\right)/n$, obtain

$$\omega^2\hat{\rho} \simeq -\frac{1}{4\pi}\nabla^2\left(\hat{\mathbf{B}}\cdot\mathbf{B}\right). \tag{22}$$

Combining this with Eq. (21) we arrive at the mode dispersion equation indicating that $\omega^2 = \left(\mathrm{V}_{Am}m^0/r_0\right)^2 + \left(\delta\omega^2\right)_1 + \left(\delta\omega^2\right)_2$, where $\left(\delta\omega^2\right)_2$ can be evaluated referring, for simplicity, to the surface $r = r_0 \simeq r_0^0$ from the solution of the following ballooning equation

$$\left(\delta\omega^2\right)_2\tilde{\rho}\left(r_0,\theta\right) \simeq -\frac{\bar{\mathrm{V}}_{Am}^2}{\left(qR_0\right)^2}\left(\frac{d^2\tilde{\rho}}{d\theta^2}\right) - \mathrm{V}_{Am}^2\left[2\left(\frac{m^0}{r_0}\right)^2\frac{r_0}{R_0}\left(1-\cos\theta\right)\right]\tilde{\rho}\left(r_0,\theta\right) \simeq 0. \tag{23}$$

This indicates that the mode is localized over a relatively small angle $\Delta\theta$, around $\theta = 0$, that is

$$\Delta\theta \sim \frac{1}{\left(qm^0\right)^{1/2}}\left(\frac{r_0}{R_0}\right)^{1/4} < 1. \tag{24}$$

Then the solution of Eq. (23) is

$$\tilde{\rho}\left(r_0,\theta\right) \simeq \tilde{\tilde{\rho}}\left(r_0\right)\exp\left(-\sigma\frac{\theta^2}{2}\right) \tag{25}$$

where

$$\sigma^2 = \left(m^0 q\right)^2\frac{R_0}{r_0} \tag{26}$$

and

$$\left(\delta\omega^2\right)_2 = \left(\frac{\mathrm{V}_{Am}}{qR_0}\right)^2. \tag{27}$$

Consequently, the distance along a magnetic field line over which the mode is localized is

$$L_{\|} \sim qR_0\frac{\Delta\theta}{2\pi}. \tag{28}$$

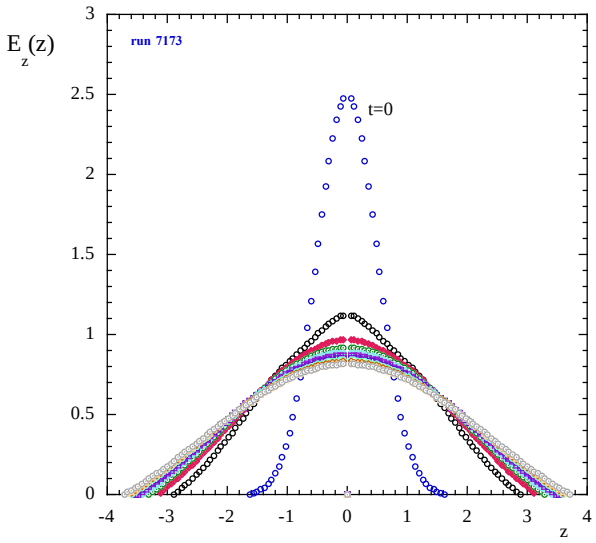

FIG.1 Ballooning mode evolution resulting from (damping) mode-particle resonances with a Maxwellian distribution. The considered ballooning mode profile is represented by Eq. (23). Courtesy of A. Cardinali]

Assuming that the α - particle density is relatively small we refer to Eq. (22) and extend it by adding the contribution of $\hat{\mathbf{P}}_\alpha$, the perturbed α - particle pressure tensor. Clearly, this can be derived from the distribution function $\hat{f}_\alpha$ based on an unperturbed $f_\alpha\left(r_0, \mathrm{v}_\perp^2, \mathrm{v}_\parallel\right)$. Considering the symmetry in θ of the driving factors of the perturbed $\hat{f}_\alpha$ (see Appendix), this can be split into an even component of θ, $\hat{f}_{\alpha-even}$, and an odd component $\hat{f}_{\alpha-odd}$. Then the mode-particle resonance condition is [see Eq. (A-9)]

$$0=\left[\left(\delta\omega_\alpha\right)-\frac{r_0}{2R_0}\theta^2\Omega_\alpha\right]+\mathrm{v}_\parallel^2\frac{1}{\left(q_0R_0\right)^2}\frac{1}{G_\alpha}\frac{dG_\alpha}{d\theta}\left\{\left[\left(\delta\omega_\alpha\right)-\frac{r_0}{2R_0}\theta^2\Omega_\alpha\right]^{-1}\frac{dG_\alpha}{d\theta}\right\}, \qquad (29)$$

where $G_\alpha\left(\theta^2\right)$ represents the ballooning profile of $\hat{f}_{\alpha-even}$. As an example, if $G_\alpha=\exp\left[-\theta^2/\left(2\left|\Delta\theta\right|^2\right)\right]$,

$$\frac{1}{G_\alpha}\frac{d^2G_\alpha}{d\theta^2}=-\frac{1}{\left|\Delta\theta\right|^2}\left(1-\frac{\theta^2}{\left|\Delta\theta\right|^2}\right).$$

For $\left|\delta\omega_\alpha\right|>>\left(r_0/R_0\right)\Omega_\alpha\theta^2$ and remembering that $\left|k_\parallel\right|$ can be represented by $\left|\theta\right|/\left[\left|\Delta\theta\right|^2 q_0R_0\right]$, we would have, instead of Eq. (29),

$$\left(\delta\omega_\alpha\right)^2-\mathrm{v}_\parallel^2\left(\left|k_\parallel\right|_{\max}^2-\left|k_\parallel\right|^2\right)=0. \qquad (30)$$

Then, if we define

$$\left(\delta\mathrm{V}_{ph}\right)\equiv\left(\delta\omega_\alpha\right)\left(q_0R_0\left|\Delta\theta\right|\right),$$

the resonant $v_{||}$ is given by

$$v_{||}^2\big)_{\mathrm{Res}} = \left(\delta V_{ph}\right)^2 \frac{1}{1-\theta^2/\left|\Delta\theta\right|^2}\,. \tag{31}$$

Considering the mode-particle resonance conditions represented by Eq. (29) it is clear that the most effective damping of the mode should correspond to deuteron velocities that are as close as possible to V_α but not so close that the resonating particle densities are too small, as in the case of particles far out in the tail of a Maxwellian distribution. Thus, a simple mathematical model incorporating these two requirements indicates that the resonant velocities, for most effective damping, corresponds to a fraction of V_α that is in the tail of the deuteron distribution. This is consistent with the experimental observation reported in Ref [10].

7. EVOLUTION OF BALLOONING MODES

Since the considered mode is contained (standing and localized) in the radial direction [8], this feature should prevent it from transporting its energy toward the wall surrounding the plasma. The other important feature is that the mode is of the ballooning type along the magnetic field and as such it can be viewed as a superposition of modes with the same frequency but propagating along the field with different phase velocities [2]. In this case the relevant mode-particle interactions that can produce damping or growth of the mode can affect the height and the width (along the magnetic field) of the mode ballooning amplitude.

Referring to the combination of growth and damping resulting from the interaction of the considered modes with the reaction products and the fusing nuclei, we may expect that the modes will evolve to become purely oscillatory where the growth and damping rates compensate each other. We expect also that the mode radial profile will change during its evolution as shown by the following analysis referring to the case where damping prevails. An oscillatory ballooning mode viewed as a superposition of standing modes having the same frequencies and involving a continuous spectrum of the relevant phase velocities [2], can be represented by

$$\hat{n} \propto \exp\left[-\frac{\theta^2}{2\left(\Delta\theta\right)^2} - i\omega t\right] \propto \exp\left[-\frac{l^2}{2\left(\Delta l\right)^2} - i\omega t\right], \tag{32}$$

where $\left(\Delta\theta\right)^2 < 1$ and $l = R_0 q_0 \theta$. Thus, the superposed waves have the form

$$\exp\left[-2k_l^2\left(\Delta l\right)^2 - i\left(\omega t - k_l l\right)\right]. \tag{33}$$

If we consider the case analyzed in Section 6, the relevant mode-particle resonance condition, for $\left|\delta\omega_\alpha\right| >> \left(r_0/R_0\right)\left|\Delta\theta\right|^2 \Omega_\alpha$, is

$$\left(\delta\omega_\alpha\right)^2 - \left(k_l v_{||}\right)^2 = 0\,. \tag{34}$$

Returning to the simpler case where $\omega = \omega_0 - i\gamma_d\left(k_l^2\right)$ and $\gamma_d > 0$, if the following model for the damping rate corresponding to all values of k_l is assumed

$$\gamma_d\left(k_l^2\right)=2\bar{\gamma}k_l^2\left(\Delta l\right)^2, \tag{35}$$

we find

$$\hat{n}\propto\frac{1}{\left(\Delta l\right)\left(1+\bar{\gamma}t\right)^{1/2}}\exp\left[-\frac{l^2}{2\left(\Delta l\right)^2\left(1+\bar{\gamma}t\right)}-i\omega_0 t\right]. \tag{36}$$

Clearly, this indicates that the resulting mode profile becomes broadened and lowered as t increases.

Starting from an initial $\left(t=0\right)$ mode profile represented by Eq. (25) an accurate numerical analysis (see Fig. 1) of the mode profile evolution has been carried out involving the relevant Landau damping with a Maxwellian distribution and it has confirmed qualitatively the results obtained with the model (35). In fact, Eq. (35) can be considered the limit of a less simplified expression such as

$$\gamma_d\left(k_l^2\right)=2\bar{\gamma}\left(\Delta l\right)^2\frac{k_l^2}{1+k_l^4/k_M^4}, \tag{37}$$

for $k_l^4<<k_M^4$. Since the process of transferring energy from populations with high energy to populations with lower energies through the excitation of ballooning modes can avoid the inefficiencies of conventional nonlinear coupling processes [3], further numerical analysis involving resonances producing both growth and damping on components of the same ballooning mode is planned. Clearly, the indications of the analysis in Section 6 will have to be considered.

8. PLASMA FLUCTUATIONS AND POWER DENSITIES

An important question is whether the considered modes will involve acceptable plasma density fluctuations in order to transfer energy at significant rates from the α - particle population to the reacting deuterons.

We may consider $Q_\alpha^0=1\ \mathrm{MW/}m^3=J/\left(cm^3s\right)$ as a reference value for the power density of the emitted α - particles and we assume that this is also a reference value for the power density of the modes driven by their interaction with the emitted α - particles. Then, referring to a homogeneous plasma model, the corresponding mode amplitudes could be evaluated from

$$Q_\alpha\simeq\gamma_\alpha\varepsilon_W$$

where ε_W is the energy density of the modes and γ_α is the rate of energy extraction from the α - particle population, and

$$\gamma_\alpha\varepsilon_W=\gamma_\alpha\frac{\left|\hat{B}_k\right|^2}{4\pi}=2\gamma_\alpha\left|\frac{\hat{B}_k}{B}\right|^2\frac{B^2}{8\pi}. \tag{38}$$

Therefore, the plasma density fluctuations associated with the extracted power density Q_α can be estimated as

$$\left|\frac{\hat{n}_k}{n}\right|\simeq\left|\frac{\hat{B}_k}{B}\right|\simeq\left(\frac{\bar{Q}_\alpha}{2\gamma_\alpha}\right)^{1/2}\left(\frac{1.6\ T}{B}\right), \tag{39}$$

where $\bar{Q}_\alpha \equiv Q_\alpha / Q_\alpha^0$, $|\hat{n}_k|/n << 1$ and $\gamma_\alpha << \Omega_\alpha \simeq 2\times 10^8 \left(B/10\ T\right) rad/s$. Thus, if $\bar{Q}_\alpha \simeq 1$, $B \simeq 10\ T$ and $2\gamma_\alpha \simeq 10^4 s$, $|\hat{n}_k / n| \simeq 1.6\times 10^{-3}$ that is a modest value. Clearly, an estimate of γ_α, associated with the resonance (29), will depend on the details of the considered α - particle distribution. The advantage of adopting high magnetic fields, for a fixed value of $\bar{Q}_\alpha / \gamma_\alpha$, is clear from Eq. (39). When all the energy extracted from the α - population is transferred to the deuterons we have

$$Q_\alpha = P_{abs} = \gamma_D \varepsilon_W \tag{40}$$

where γ_D is the relevant damping rate.

As a start, we may assume a Maxwellian distribution for the deuterons and consider $k_\perp^2 \rho_D^2 << 1$ where $\rho_D^2 = 2T_D / \left(m_D \Omega_D^2\right)$ for the relevant perturbations. Given the characteristics of the mode-particle resonant interactions discussed earlier, one of the difficulty of relying on a homogeneous plasma model, to have an estimate of γ_D, is that the result depends on a significant choice for a representative value of $k_\parallel$. In fact, the mode-particle resonances represented by Eq. (29) depends on θ and the consequence of this is that the mode profile, along the magnetic field, can change as a function of time as shown by the analysis of Section 7. Therefore, the definitions of γ_α and γ_D will have to be reformulated accordingly. In particular, referring for simplicity to Eq. (30) and considering that superthermal deuterons should be involved in absorbing the mode energy, we may take

$$\left(\delta \mathrm{V}_{ph}\right)^2 \simeq \alpha_{ST} \left(2T_D / m_D\right) \tag{41}$$

with $\alpha_{ST} \geq 1$. In this case the corresponding mode amplitude is its maximum, as $\mathrm{v}_\parallel\big)_{\mathrm{Res}}^D = \left(\delta \mathrm{V}_{ph}\right)$, is reached at $\theta = 0$. On the other hand, if $\mathrm{V}_\alpha^2 >> \left(\delta \mathrm{V}_{ph}\right)^2$ a significant resonance with the α - particle population is reached for θ^2 near $|\Delta\theta|^2$.

Finally, we observe that when considering higher harmonics of Ω_α the mode-particle resonance condition (29) is replaced by

$$\left(\omega - p^0 \Omega_\alpha\right)^2 - \mathrm{v}_\parallel^2 \frac{1}{\left(q_0 R_0\right)^2 |\Delta\theta|^2} \left(1 - \frac{\theta^2}{|\Delta\theta|^2}\right) = 0 . \tag{42}$$

Clearly, the coupling of higher harmonics with the lowest harmonic $\left(p^0 = 1\right)$ deserves to be taken into consideration in view of the features of the perturbed deuteron density and for $\left(k_\perp \rho_D\right)^2 << 1$.

9. RELEVANT EXPERIMENTAL OBSERVATIONS

Results that are relevant to the theory described in the previous sections have been obtained by a series of experiments [10] carried out on magnetically confined plasmas with a combined mirror – FRC confinement configuration. These involved Deuterium plasmas with relatively low temperatures in which a Hydrogen neutral beam with relatively high energy (30 keV) was injected.

A large increase of neutron emission, due to DD reactions, was observed. This is clearly due to a collective mode driven by high energy protons and supplying energy to the tail of the (energy) distribution of the reacting nuclei. A coherent mode with the Deuteron cyclotron frequency was observed at the same time. Differently from the theory involving DT plasmas, the cyclotron frequency of the high energy population is larger than that of the reacting nuclei. On the other hand, considering that most of the area of the transverse cross section of the plasma column is subject to an axisymmetric magnetic field distribution of the mirror kind, the emergence of a ballooning mode [11] of the kind analyzed in the previous section can be envisioned. In this case the magnetic field near $z = 0$, z being the symmetry axis would be of the form $B \simeq B_0 \left(1 + l^2 / L^2\right)$, l being the distance along a given field line. Then the analysis summarized in Section 6 can be extended [12] to cover this case. Clearly, it would be desirable to conduct parallel experiments on plasmas with different magnetic confinement configurations.

The first set of experiments with DT plasmas carried out by the JET facility [9] revealed significant rate of e.m. radiation emission from the lowest to high harmonics of Ω_α. Assuming that modes of the kind analyzed here were excited, a coupling to e.m. modes with observed frequency and propagating away from the plasma column should be considered. Since neutrons of non-thermal origin have also been observed it is conceivable that a fraction of them could be associated with the excitation of relevant collective modes.

10. FINAL CONSIDERATIONS

Therefore, by identifying and possibly controlling the modes that can increase the reaction rates, for a given temperature of the electron population, can lead to new perspectives that include D-T ignition under less restrictive conditions than those usually assumed, utilizing high magnetic field experiments to reach significant burn conditions with D-D catalyzed reaction, etc. On the other hand, new experiments will be needed to ascertain the excitation of the considered modes – an objective that can be pursued even with plasmas that do not contain tritium, as indicated earlier. Another issue that needs consideration is that of gaining some control on the process by which the amplitudes of these modes are limited. A damping on a region of the distribution in phase space of the reacting nuclei which can maximize the plasma reactivity is certainly desirable. In this context, the technology developed, and the expertise gained in introducing of Ion Cyclotron Resonant Heating (ICRH) systems, may make it possible to interact from outside the plasma column with the considered modes without the high-power requirements associated with "conventional" ion cyclotron heating.

ACKNOWLEDGEMENTS

We are indebted to A. Cardinali and V. Ricci for their contributions to the first phase [12] of this ongoing work and for their continuing concern. Sponsored in part by the Kavli Foundation (through MIT) and by CNR (Consiglio Nazionale delle Ricerche) of Italy.

REFERENCES

[1] COPPI, B., Non-classical transport and the 'principle of profile consistency', Comments Pl. Phys. Con. Fus. Res. 5, (1980) 261.

[2] COPPI, B., Gravitation by nonaxisymmetric rotating objects and generation of high-energy particle populations, Plasma Phys. Rep. 45, (2019) 438.
[3] COPPI, B., ROSENBLUTH, M.N., and SUDAN, R. N., Non-linear interactions of positive and negative energy modes in rarefied plasmas, Ann. Phys. 55, (1969) 207.
[4] COPPI, B., ROSENBLUTH, M.N., YOSHIKAWA, S., Localized (ballooning) modes in multipole configurations, Phys. Rev. Lett., **20**, (1968) 190.
[5] COPPI, B., Topology of ballooning modes, Phys. Rev. Lett., **39**, (1977) 939.
[6] COPPI, B., COWLEY, S., KULSRUD, R., DETRAGIACHE, P., PEGORARO, F., High-energy components and collective modes in thermonuclear plasmas Phys. Fluids, **12** (1986), 4060.
[7] ROSENBLUTH, M.N., Microinstabilities, Plasma Physics (1965), 501, Publ. I.A.E.A., Vienna (1965).
[8] COPPI, B., Origin of radiation emission induced by fusion reaction products, Phys. Lett. A **172**, (1993) 439.
[9] JET Team, Fusion energy production from a deuterium-tritium plasma in the JET tokamak, Nucl. Fus. **32**, (1992) 187.
[10] MAGEE, R. M., NECAS, A., CLARY, R., KOREPANOV, S., NICKS, S., ROCHE, T., THOMPSON, M. C., BINDERBAUER, M. W., TAJIMA, T., Direct observation of ion acceleration from a beam-driven wave in a magnetic fusion experiment, Nature Phys. **15**, (2019) 281.
[11] COPPI, B., Energy cascading through soliton-like modes in high energy plasmas, MIT/LNS Report HEP 2023/1, Cambridge, MA (2023).
[12] COPPI, B., BASU, B., CARDINALI, A., Fusion burn conditions for non-thermal plasmas, Paper Th/P, Proceedings of the 2021 Fusion Energy Conference Publ. I.A.E.A., Vienna, (2021).

APPENDIX

Driven Distribution Functions

Referring at first to the α - particle population we start from the linearized collisionless equation

$$\left[\frac{\partial}{\partial t}+\mathbf{v}\cdot\nabla+\frac{q_\alpha}{m_\alpha c}(\mathbf{v}\times\mathbf{B})\cdot\frac{\partial}{\partial\mathbf{v}}\right]\hat{f}_\alpha(\mathbf{r},\mathbf{v},t)+\frac{q_\alpha}{m_\alpha}\left(\hat{\mathbf{E}}+\frac{\mathbf{v}\times\hat{\mathbf{B}}}{c}\right)\cdot\frac{\partial}{\partial\mathbf{v}}f_\alpha(\mathbf{v})=0\,, \qquad \text{(A-1)}$$

and refer to the coordinates $\mathrm{v}_{\|}$ and $\mathrm{v}_{\perp}$ in velocity space, where $\mathrm{v}_{\|}\equiv\mathbf{v}\cdot\mathbf{B}/B$, $\mathbf{v}_{\perp}\equiv\mathbf{v}-\mathrm{v}_{\|}\mathbf{B}/B$, $\mathrm{v}_r=\mathrm{v}_{\perp}\cos\bar{\varphi}$, $\mathrm{v}_\theta=\mathrm{v}_{\perp}\sin\bar{\varphi}$, $\mathrm{v}_{\perp}=\sqrt{\mathrm{v}_r^2+\mathrm{v}_\theta^2}$ and $\bar{\varphi}=\tan^{-1}(\mathrm{v}_\theta/\mathrm{v}_r)$. Then

$$\mathbf{v}\cdot\nabla\hat{f}_\alpha=i\frac{m^0}{r_0}\mathrm{v}_{\perp}\sin\bar{\varphi}\,\hat{f}_\alpha+\mathrm{v}_{\|}\frac{\partial}{\partial l}\hat{f}_\alpha$$

$$\frac{q_\alpha}{m_\alpha c}(\mathbf{v}\times\mathbf{B})\cdot\frac{\partial}{\partial\mathbf{v}}\hat{f}_\alpha=-\Omega_\alpha\frac{\partial}{\partial\bar{\varphi}}\hat{f}_\alpha$$

$$\hat{\mathbf{E}}\cdot\frac{\partial}{\partial\mathbf{v}}f_\alpha(\mathrm{v}_{\perp},\mathrm{v}_{\|})=2\hat{\mathbf{E}}_{\perp}\cdot\mathbf{v}_{\perp}\frac{\partial}{\partial\mathrm{v}_{\perp}^2}f_\alpha+\hat{E}_{\|}\frac{\partial}{\partial\mathrm{v}_{\|}}f_\alpha$$

where $\partial/\partial l\simeq\left[1/(q_0R_0)\right]\partial/\partial\theta$. Moreover

$$\left(\mathbf{v}\times\hat{\mathbf{B}}\right)\cdot\frac{\partial}{\partial\mathbf{v}}f_\alpha\left(\mathrm{v}_\perp,\mathrm{v}_\parallel\right)=0$$

if we assume for simplicity that f_α is isotropic. Consequently, Eq. (A-1) reduces to

$$\begin{aligned}&-i\omega\hat{f}_\alpha+i\frac{m^0}{r_0}\mathrm{v}_\perp\sin\bar{\varphi}\,\hat{f}_\alpha+\mathrm{v}_\parallel\frac{\partial}{\partial l}\hat{f}_\alpha-\Omega_\alpha\frac{\partial}{\partial\bar{\varphi}}\hat{f}_\alpha\\&=-\frac{q_\alpha}{m_\alpha}\left\{\left(\hat{E}_r\cos\bar{\varphi}+\hat{E}_\theta\sin\bar{\varphi}\right)\frac{\partial}{\partial\mathrm{v}_\perp}f_\alpha+\hat{E}_\parallel\frac{\partial}{\partial\mathrm{v}_\parallel}f_\alpha\right\}.\end{aligned}\tag{A-2}$$

We define

$$\hat{f}_\alpha\left(l,\mathrm{v}_\parallel,\mathrm{v}_\perp,\bar{\varphi}\right)\equiv\hat{g}_\alpha\left(l,\mathrm{v}_\parallel,\mathrm{v}_\perp,\bar{\varphi}\right)\exp\left(-i\mu_\alpha\cos\bar{\varphi}\right)\tag{A-3}$$

where $\mu_\alpha\equiv\left(m^0/r_0\right)\left(\mathrm{v}_\perp/\Omega_\alpha\right)$ and find

$$\begin{aligned}&\left(-i\omega+\mathrm{v}_\parallel\frac{\partial}{\partial l}\right)\hat{g}_\alpha-\Omega_\alpha\frac{\partial}{\partial\bar{\varphi}}\hat{g}_\alpha\\&=-\frac{q_\alpha}{m_\alpha}\exp\left(i\mu_\alpha\cos\bar{\varphi}\right)\left\{\left(\hat{E}_r\cos\bar{\varphi}+\hat{E}_\theta\sin\bar{\varphi}\right)\frac{\partial}{\partial\mathrm{v}_\perp}f_\alpha+\hat{E}_\parallel\frac{\partial}{\partial\mathrm{v}_\parallel}f_\alpha\right\}\end{aligned}\tag{A-4}$$

Next, use $\hat{g}_\alpha\left(l,\mathrm{v}_\parallel,\mathrm{v}_\perp,\bar{\varphi}\right)=\sum_{n=-\infty}^{+\infty}\hat{\hat{g}}_{\alpha,n}\left(l,\mathrm{v}_\parallel,\mathrm{v}_\perp\right)\exp\left(-in\bar{\varphi}\right)$ in Eq. (A-4) and obtain

$$\begin{aligned}&\sum_{n=-\infty}^{+\infty}\left(-i\omega+in\Omega_\alpha+\mathrm{v}_\parallel\frac{\partial}{\partial l}\right)\hat{\hat{g}}_{\alpha,n}\left(l,\mathrm{v}_\parallel,\mathrm{v}_\perp\right)\exp\left(-in\bar{\varphi}\right)\\&=-\frac{q_\alpha}{m_\alpha}\exp\left(i\mu_\alpha\cos\bar{\varphi}\right)\left\{\left(\hat{E}_r\cos\bar{\varphi}+\hat{E}_\theta\sin\bar{\varphi}\right)\frac{\partial}{\partial\mathrm{v}_\perp}f_\alpha+\hat{E}_\parallel\frac{\partial}{\partial\mathrm{v}_\parallel}f_\alpha\right\}\end{aligned}\tag{A-5}$$

Now we use the following expressions

$$\begin{aligned}&\sum_{n=-\infty}^{+\infty}i^nJ_n\left(\mu_\alpha\right)\exp\left(-in\bar{\varphi}\right)=\exp\left(i\mu_\alpha\cos\bar{\varphi}\right),\\&\sum_{n=-\infty}^{+\infty}i^nnJ_n\left(\mu_\alpha\right)\exp\left(-in\bar{\varphi}\right)=\mu_\alpha\sin\bar{\varphi}\exp\left(i\mu_\alpha\cos\bar{\varphi}\right),\\&\sum_{n=-\infty}^{+\infty}i^nJ_n'\left(\mu_\alpha\right)\exp\left(-in\bar{\varphi}\right)=i\cos\bar{\varphi}\exp\left(i\mu_\alpha\cos\bar{\varphi}\right),\end{aligned}\tag{A-6}$$

and obtain from Eq. (A-5),

$$\begin{aligned}&\sum_{n=-\infty}^{+\infty}\left(-i\omega+in\Omega_\alpha+\mathrm{v}_\parallel\frac{\partial}{\partial l}\right)\hat{\hat{g}}_{\alpha,n}\exp\left(-in\bar{\varphi}\right)\\&=i\frac{q_\alpha}{m_\alpha}\sum_{n=-\infty}^{+\infty}i^n\left\{\left[J_n'\left(\mu_\alpha\right)\hat{E}_r+i\frac{n}{\mu_\alpha}J_n\left(\mu_\alpha\right)\hat{E}_\theta\right]\frac{\partial}{\partial\mathrm{v}_\perp}f_\alpha+iJ_n\left(\mu_\alpha\right)\hat{E}_\parallel\frac{\partial}{\partial\mathrm{v}_\parallel}f_\alpha\right\}\exp\left(-in\bar{\varphi}\right).\end{aligned}\tag{A-7}$$

Thus

$$\left(-i\omega + in\Omega_\alpha + \mathrm{v}_\parallel \frac{\partial}{\partial l}\right)\hat{\hat{g}}_{\alpha,n}\left(l,\mathrm{v}_\parallel,\mathrm{v}_\perp,\mathbf{r}_\perp\right)$$
$$= \frac{q_\alpha}{m_\alpha} i^{n+1}\left\{\left[J_n'\left(\mu_\alpha\right)\hat{E}_r + i\frac{n}{\mu_\alpha}J_n\left(\mu_\alpha\right)\hat{E}_\theta\right]\frac{\partial}{\partial \mathrm{v}_\perp} f_\alpha + iJ_n\left(\mu_\alpha\right)\hat{E}_\parallel \frac{\partial}{\partial \mathrm{v}_\parallel} f_\alpha\right\}. \quad \text{(A-8)}$$

In particular for $n=1$ and $\omega = \Omega_\alpha + \delta\omega_\alpha$

$$\left(-i\delta\omega_\alpha + \mathrm{v}_\parallel \frac{\partial}{\partial l}\right)\tilde{\hat{g}}_{\alpha,1}\left(l,\mathrm{v}_\parallel,\mathrm{v}_\perp\right)$$
$$= -\frac{q_\alpha}{m_\alpha}\left\{\left[J_1'\left(\mu_\alpha\right)\tilde{E}_r + i\frac{1}{\mu_\alpha}J_1\left(\mu_\alpha\right)\tilde{E}_\theta\right]\frac{\partial}{\partial \mathrm{v}_\perp} f_\alpha + iJ_1\left(\mu_\alpha\right)\tilde{E}_\parallel \frac{\partial}{\partial \mathrm{v}_\parallel} f_\alpha\right\}. \quad \text{(A-9)}$$

Now if we separate $\tilde{\hat{g}}_{\alpha,1}$ into an even and odd functions and take into account the parity of the r.h.s. of Eq. (A-8) we arrive at the mode-particle resonance (8-4).

Referring to Eq. (A-3) we have

$$\hat{f}_\alpha\left(l,\mathrm{v}_\parallel,\mathrm{v}_\perp,\bar{\varphi}\right) = \sum_{n=-\infty}^{+\infty}\hat{\hat{g}}_{\alpha,n}\left(l,\mathrm{v}_\parallel,\mathrm{v}_\perp\right)\exp\left(-in\bar{\varphi} - i\mu_\alpha\cos\bar{\varphi}\right). \quad \text{(A-10)}$$

When the expression

$$\exp\left(-i\mu_\alpha\cos\bar{\varphi}\right) = \sum_{m=-\infty}^{+\infty}\left(-i\right)^m J_m\left(\mu_\alpha\right)\exp\left(im\bar{\varphi}\right) \quad \text{(A-11)}$$

is used, Eq. (A-10) gives

$$\int d\bar{\varphi}\,\hat{f}_\alpha\left(l,\mathrm{v}_\parallel,\mathrm{v}_\perp,\bar{\varphi}\right) = 2\pi\sum_{n=-\infty}^{+\infty}\left(-i\right)^n J_n\left(\mu_\alpha\right)\hat{\hat{g}}_{\alpha,n}\left(l,\mathrm{v}_\parallel,\mathrm{v}_\perp\right), \quad \text{(A-12)}$$

where $\hat{\hat{g}}_{\alpha,n}\left(l,\mathrm{v}_\parallel,\mathrm{v}_\perp\right)$ is determined by Eq. (A-8).

For the modes that we consider we may take $\hat{E}_\varphi = 0$, $\hat{\mathbf{E}}_\perp \simeq \hat{E}_r\mathbf{e}_r$ and $\left(\omega/c\right)\hat{B}_\varphi \simeq -i\left(m^0/r_0\right)\hat{E}_r$. Since $\hat{B}_\varphi / B \propto \hat{n}/n$, $\hat{B}_\varphi$ and $\hat{E}_r$ are even functions of θ.

To assess the effect of the mode-particle resonance for the deuteron population we consider, for simplicity, the homogeneous plasma model. In this case, we refer to Eq. (A-8), where we take $\tilde{E}_z = 0$, $\partial/\partial l = ik_\parallel$, and find $\tilde{f}_D$, the perturbed deuteron distribution function, as

$$\tilde{f}_D = -\frac{e}{m_D}\sum_{n=-\infty}^{+\infty} i^n \frac{\exp\left(-in\bar{\varphi} - i\mu_D\cos\bar{\varphi}\right)}{\omega - n\Omega_D - k_\parallel \mathrm{v}_\parallel}\left[J_n'\left(\mu_D\right)\tilde{E}_x + i\frac{n}{\mu_D}J_n\left(\mu_D\right)\tilde{E}_y\right]\frac{\partial}{\partial \mathrm{v}_\perp} f_D^M \quad \text{(A-13)}$$

where $\mu_D \equiv k_y \mathrm{v}_\perp / \Omega_D$. Using the expression given by Eq. (A-11), we derive the perturbed density $\tilde{n}_D$ as

$$\tilde{n}_D \simeq \frac{\pi e}{k_y T_D}\int d\mathrm{v}_\perp^2 d\mathrm{v}_\parallel f_D^M \times\left\{\mu_D\left[J_0(\mu_D)J_0'(\mu_D)+\frac{\Omega_D}{\delta\omega_\alpha - k_\parallel \mathrm{v}_\parallel}J_1(\mu_D)J_1'(\mu_D)\right]\tilde{E}_x + i\frac{\Omega_D}{\delta\omega_\alpha - k_\parallel \mathrm{v}_\parallel}J_1^2(\mu_D)\tilde{E}_y\right\}, \tag{A-14}$$

where f_D^M is the deuteron Maxwellian distribution. It may be verified that, in the limits $\mu_D << 1$ and $\delta\omega_\alpha >> k_\parallel \mathrm{v}_\parallel$, Eq. (A-14) for $\tilde{n}_D$ agrees with the result that is obtained from the fluid equations (particle and momentum conservation equations). Thus, for $b_D \equiv k_y^2 T_D / \left(m_D \Omega_D^2\right) << 1$ and following standard procedures,

$$\mathrm{Im}\left(\tilde{n}_D\right) \simeq -\left|\tilde{n}_D\right| \mathrm{Im} W_D(\lambda), \tag{A-15}$$

where $\mathrm{Im} W_D(\lambda) = \sqrt{\pi}\lambda \exp\left(-\lambda^2\right)$ and $\lambda \equiv \delta\omega_\alpha / \left|k_\parallel \mathrm{V}_{th}\right|_D$.